Preclinical Development

Molecular Cancer Therapeutics

NMS-P937, an Orally Available, Specific Small-Molecule Polo-like Kinase 1 Inhibitor with Antitumor Activity in Solid and Hematologic Malignancies

Barbara Valsasina[1], Italo Beria[1], Cristina Alli[1], Rachele Alzani[1], Nilla Avanzi[1], Dario Ballinari[1], Paolo Cappella[1], Michele Caruso[1], Alessia Casolaro[1], Antonella Ciavolella[1], Ulisse Cucchi[1], Anna De Ponti[1], Eduard Felder[1], Francesco Fiorentini[2], Arturo Galvani[1], Laura M. Gianellini[1], Maria L. Giorgini[1], Antonella Isacchi[1], Jaqueline Lansen[2], Enrico Pesenti[1], Simona Rizzi[1], Maurizio Rocchetti[2], Francesco Sola[1], and Jürgen Moll[1]

Abstract

Polo-like kinase 1 (PLK1) is a serine/threonine protein kinase considered to be the master player of cell-cycle regulation during mitosis. It is indeed involved in centrosome maturation, bipolar spindle formation, chromosome separation, and cytokinesis. PLK1 is overexpressed in a variety of human tumors and its overexpression often correlates with poor prognosis. Although five different PLKs are described in humans, depletion or inhibition of kinase activity of PLK1 is sufficient to induce cell-cycle arrest and apoptosis in cancer cell lines and in xenograft tumor models. NMS-P937 is a novel, orally available PLK1-specific inhibitor. The compound shows high potency in proliferation assays having low nanomolar activity on a large number of cell lines, both from solid and hematologic tumors. NMS-P937 potently causes a mitotic cell-cycle arrest followed by apoptosis in cancer cell lines and inhibits xenograft tumor growth with clear PLK1-related mechanism of action at well-tolerated doses in mice after oral administration. In addition, NMS-P937 shows potential for combination in clinical settings with approved cytotoxic drugs, causing tumor regression in HT29 human colon adenocarcinoma xenografts upon combination with irinotecan and prolonged survival of animals in a disseminated model of acute myelogenous leukemia in combination with cytarabine. NMS-P937, with its favorable pharmacologic parameters, good oral bioavailability in rodent and nonrodent species, and proven antitumor activity in different preclinical models using a variety of dosing regimens, potentially provides a high degree of flexibility in dosing schedules and warrants investigation in clinical settings. *Mol Cancer Ther; 11(4); 1006–16. ©2012 AACR.*

Introduction

Mitotic cell-cycle progression is tightly regulated through reversible covalent protein phosphorylation events coordinated by regulatory kinases, including members of the polo subfamily (1). Among the 5 human polo-like kinase (PLK) isoforms (PLK1–5), PLK1 is the best characterized and is recognized to be a key component of the cell-cycle control machinery with important roles in mitotic entry, centrosome duplication, bipolar mitotic spindle formation, transition from metaphase to anaphase, cytokinesis, and maintenance of genomic stability (2). PLK1 is frequently found to be overexpressed in numerous tumor types including pancreatic (3), colon (4), prostate (5), ovary (6), breast (7), head and neck (8), anaplastic thyroid (9) carcinomas, melanoma (10), and in a set of hematologic malignancies comprising acute myelogenous leukemia (AML; refs. 11, 12), and non-Hodgkins lymphoma (13), with overexpression often correlated with poor prognosis. Interference with PLK1 activity and/or function by a variety of methods including antisense oligonucleotides (14), short interfering RNA (15), and proteins encoding dominant-negative PLK1 (16) results in tumor cell apoptosis in culture and *in vivo*. Moreover normal cells have been described to better tolerate PLK1 depletion as compared with tumor cells (17). These data support PLK1 as a potentially valuable target for anticancer drug development. Although depletion of PLK1 is sufficient to induce a G_2–M cell-cycle block, less is known concerning the physiologic roles of PLK2 and PLK3, the members of the family with highest similarity to PLK1. In contrast to PLK1, they are expressed in nonproliferating differentiated postmitotic cells including neurons (18). Hence, a PLK1 selective inhibitor might be expected to have a superior safety profile compared with pan-PLK inhibitors.

Authors' Affiliations: [1]Nerviano Medical Sciences S.r.l.; and [2]Accelera S.r.l., Nerviano, Milan, Italy

Note: Supplementary material for this article is available at Molecular Cancer Therapeutics Online (http://mct.aacrjournals.org/).

Corresponding Author: Barbara Valsasina, Biotechnology Department, BU Oncology, Nerviano Medical Sciences S.r.l., Viale Pasteur 10, Nerviano, MI 20014, Italy. Phone: 39-0331-581178; Fax: 39-0331-581267; E-mail: barbara.valsasina@nervianoms.com

doi: 10.1158/1535-7163.MCT-11-0765

Because of its essential role in cell proliferation there are intense efforts to identify and develop small-molecule inhibitors of PLK1 and indeed different compounds are currently under clinical investigation (19).

In our effort to develop selective small-molecule PLK1 inhibitors, we previously described a novel series of ATP-competitive 4,5-dihydro-1*H*-pyrazolo[4,3-*h*]quinazoline derivatives (20, 21). Here, we report the *in vitro* activity and *in vivo* pharmacokinetic, pharmacodynamic, and efficacy profiles of NMS-P937. This compound shows excellent selectivity within the PLK family and among a large panel of protein kinases and good antiproliferative activity on tumor cell lines, which is accompanied by an unambiguous PLK1-related mechanism of action. *In vivo* NMS-P937 shows antitumor activity correlated with clear biomarker modulation and good tolerability in different xenograft models as single agent or in combination with registered cytotoxic drugs. These properties make NMS-P937 an interesting compound, which is currently being explored in clinical trials.

Materials and Methods

Chemicals

NMS-P937 was synthesized at Nerviano Medical Sciences, S.r.l. (Nerviano, MI, Italy). CPT-11 (Irinotecan, Camptosar) was purchased from Pfizer, Cytarabine was purchased from Hospira.

Biochemical kinase inhibition assays

Inhibition of kinase activity by NMS-P937 was assessed with an anion exchanger (Dowex 1 × 8 resin 200–400 mesh)-based assay as previously described (21).

Cell culture

Human cancer cell lines were obtained either from the American Type Culture Collection (ATCC) or from the European Collection of Cell Culture. Cells were maintained in the media and serum concentrations recommended by the suppliers, supplemented with 1% penicillin-streptomycin (Sigma), in a humidified 37°C incubator with 5% CO_2.

Cell line authentication

All cell lines used in the study were profiled using DNA fingerprinting technology (AmpFlSTR Identifiler Plus PCR Amplification Kit; Applied Biosystems) according to the manufacturer's protocol. The short tandem repeat profiles of the analyzed cell lines were compared with DNA fingerprinting databases (e.g., ATCC and DMSZ). All the analyzed profiles showed a similarity higher than 80%. All cell lines used were obtained directly from the authenticated suppliers listed earlier and are routinely confirmed at 6-month intervals.

Analysis of cell proliferation

Cells were seeded into 96- or 384-well plates at densities ranging from 10,000 to 30,000/cm^2 for adherent and 100,000/mL for nonadherent cells in appropriate medium supplemented with 10% fetal calf serum. After 24 hours, cells were treated in duplicate with serial dilutions of NMS-P937, and 72 hours later, the viable cell number was assessed by the CellTiter-Glo Assay (Promega). IC_{50} values were calculated with a sigmoidal fitting algorithm (Assay Explorer MDL). Experiments were carried out independently at least twice.

Cell-based assays

NMS-P937 mechanism of action as a PLK1 inhibitor was investigated in A2780 human ovarian carcinoma cells. Cells were analyzed by Western blotting and flow cytometry, measuring cell-cycle–dependent parameters and DNA synthesis.

To investigate PLK1-specific mechanism of action, phospho-Ser46 TCTP (22) was evaluated in parallel with phospho-Ser10 Histone H3 in lysates from cells treated for 1 hour with NMS-P937 or dimethyl sulfoxide (DMSO) as a control.

Western blot analysis

Twenty micrograms of protein extract was separated by SDS-PAGE. Immunoblotting was carried out according to standard procedures, and staining was done with the corresponding antibodies recognizing. PLK1 (Zymed), phospho-Thr210 PLK1 (BD Biosciences), phospho-Ser10 Histone H3 (Upstate), phospho-Tyr15 CDK1 (Cell Signaling), phospho-Thr199 NPM (Cell Signaling), total NPM (Cell signaling), total CDK1 (Santa Cruz), PARP1 (Calbiochem), phospho-Ser46 TCTP (custom made by Zymed), and phospho-Ser139 Histone H2.X (Millipore). The SuperSignal Chemiluminescence Kit (Pierce) was used for detection.

Cell-cycle analysis

Cells were collected, fixed, and stained. Cytofluorimetric analysis was conducted using a FACSCalibur (BD Biosciences), and cell-cycle phases were calculated by ModFit 3.0 (Verity Software House) as previously described (22).

Animal efficacy studies

All procedures adopted for housing and handling of animals were in strict compliance with European and Italian Guidelines for Laboratory Animal Welfare. For carcinoma xenograft studies, 5- to 6-week-old female Hsd, athymic *nu/nu* mice (average weight, 20–22 g), were used (Harlan). HCT116, HT29, Colo205 colorectal, and A2780 ovarian human carcinoma cell lines were inoculated subcutaneously. Mice bearing a palpable tumor (100–200 mm^3) were treated with vehicle or NMS-P937 following doses and schedules indicated in Fig. 4 starting from the day after randomization. Tumor dimensions were measured regularly with Vernier calipers, and tumor growth inhibition (TGI) was calculated as previously described (23). Toxicity was evaluated on the basis of body weight reduction. For leukemia studies, 5- to 6-week-old female severe combined immunodeficient mice (SCID; average

weight, 20–22 g) were used (Harlan). The AML cell line HL-60 (5×10^6 cells) was injected subcutaneously and treatments initiated when tumor size reached 200 to 250 mm^3. Tumor dimensions and TGI were assessed as described earlier. For disseminated models, 5×10^6 AML primary cells (AML-PS), kindly provided by J. Goulay (Ospedali Riuniti Bergamo, Italy), were injected intravenously and treatments started after 2 days. Mice were monitored daily for clinical signs of disease, and the median survival time was determined for each group.

Ex vivo mechanism of action studies

A2780 tumor–bearing mice (4 per group) were treated orally with vehicle or single doses of NMS-P937 (60, 90, or 120 mg/kg). Tumors were collected at different time points after the administration and divided for immunohistochemistry and Western blot analysis.

Results

Kinase inhibition

NMS-P937 (Fig. 1) is a pyrazoloquinazoline, which potently inhibits the kinase activity of PLK1 in a biochemical assay, with an IC_{50} value of 2 nmol/L. ATP and substrate titration studies showed NMS-P937 to possess a pure ATP competitive mechanism with a reversible dissociation and no time dependency. The potency of the compound depends on ATP concentration, whereas no change in the IC_{50} value was observed upon changing the substrate concentration. Interpretation of data from a time course matrix experiment allowed determination of inhibition constant (K_i) value of about 1 nmol/L for NMS-P937 (Supplementary Fig. S1).

NMS-P937 is highly selective for PLK1 when tested on a panel of 63 protein kinases representative of the human kinome superfamily. High nanomolar activity for CK2, FLT3, and MELK was detected, whereas the compound resulted inactive on the other kinases of the panel at the highest concentration (10 μmol/L) tested (Table 1). In addition NMS-P937 is selective within the PLK family (Table 1) with a marginal activity of 48% and 40% inhibition on PLK2 and PLK3, respectively, when tested at 10 μmol/L. To better explore selectivity, NMS-P937 was screened at 2 different concentrations, 0.1 and 1 μmol/L, against a commercial panel of recombinant kinases (Kinase Profiler; Millipore). In this screen, the compound resulted to be highly selective showing residual kinase activity less than 50% in 11 of 296 kinases (including PLK1) when tested at 1 μmol/L, with PLK1 being the only kinase with 10% residual activity at 0.1 μmol/L (Supplementary Table S1).

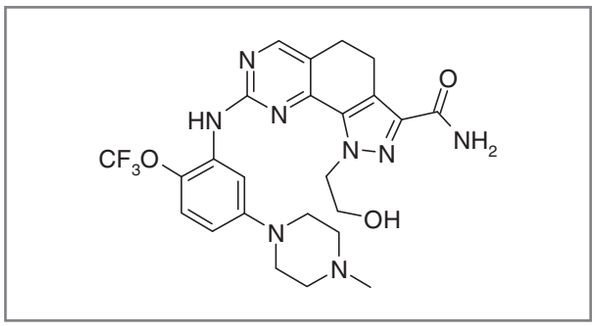

Figure 1. Chemical structure of the pyrazoloquinazoline NMS-P937.

Table 1. Biochemical potency on a panel of 63 kinases

Enzyme	IC_{50}, μmol/L	% Inhibition at 10 μmol/L
PLK1	0.002	100.0
PLK2	10	48.2
PLK3	10	40.2
FLT3	0.51	96.3
MELK	0.744	95.5
CK2	0.826	89.7

NOTE: IC50 > 10 μmol/L: ABL, ACK1, AKT1, ALK, AUR1, AUR2, BRK, BUB1, CDC7/DBF4, CDK1/CycB, CDK2/CycA, CDK2/CycE, CDK4/CycD1, CDK5/P25, CHK1, EEF2K, EGFR1, EphA2, ERK2, FGFR1, GSK3β, Haspin, IGFR1, IKK2, IR, JAK1, JAK2, JAK3, KIT, LCK, LYN, MAPKAPK2, MET, MNK2, MPS1, MST4, NEK6, NIM1, P38α, PAK4, PDGFR, PDK1, PERK, PIM1, PIM2, PKAα, PKCβ, RET, ROS, SULU1, SYK, TLK2, TRKA, TYK2, VEGFR2, VEGFR3, ZAP70.

An explanation for the excellent selectivity profile of NMS-P937 is its binding mode in the ATP pocket as evident in the X-ray cocrystal structure of the PLK1 kinase domain and NMS-P937, described by Beria and colleagues (24). Briefly, the compound binds to the ATP pocket of the PLK1 kinase domain in the active conformation (type I inhibitor) and hydrogen bonds are formed with key residues in the kinase hinge region. The 2′-trifluoromethoxy group plays a crucial role in obtaining selectivity against kinases bearing a residue bulkier than leucine in this position, such as for example Aurora-A kinase or CDK2. PLK1 selectivity with respect to PLK 2–3 is instead based on the 5′-methylpiperazine moiety that establishes a polar interaction with Glu^{140} of PLK1 (Supplementary Fig. S2). The same interaction is hampered in PLK2 and PLK3, where histidine is found in the corresponding position.

Effect on tumor cell proliferation and mechanism of action

The antiproliferative activity of NMS-P937 was tested in a 72-hour proliferation assay against a panel of 137 cell lines established from different solid tumors and a further 43 cell lines derived from leukemias and lymphomas (Supplementary Tables S2 and S3). IC_{50} values were below 100 nmol/L (Fig. 2A) for 60 of 137 cell lines and higher than 1 μmol/L for only 9 of 137 cell lines, indicating a broad spectrum of activity. NMS-P937 is also highly

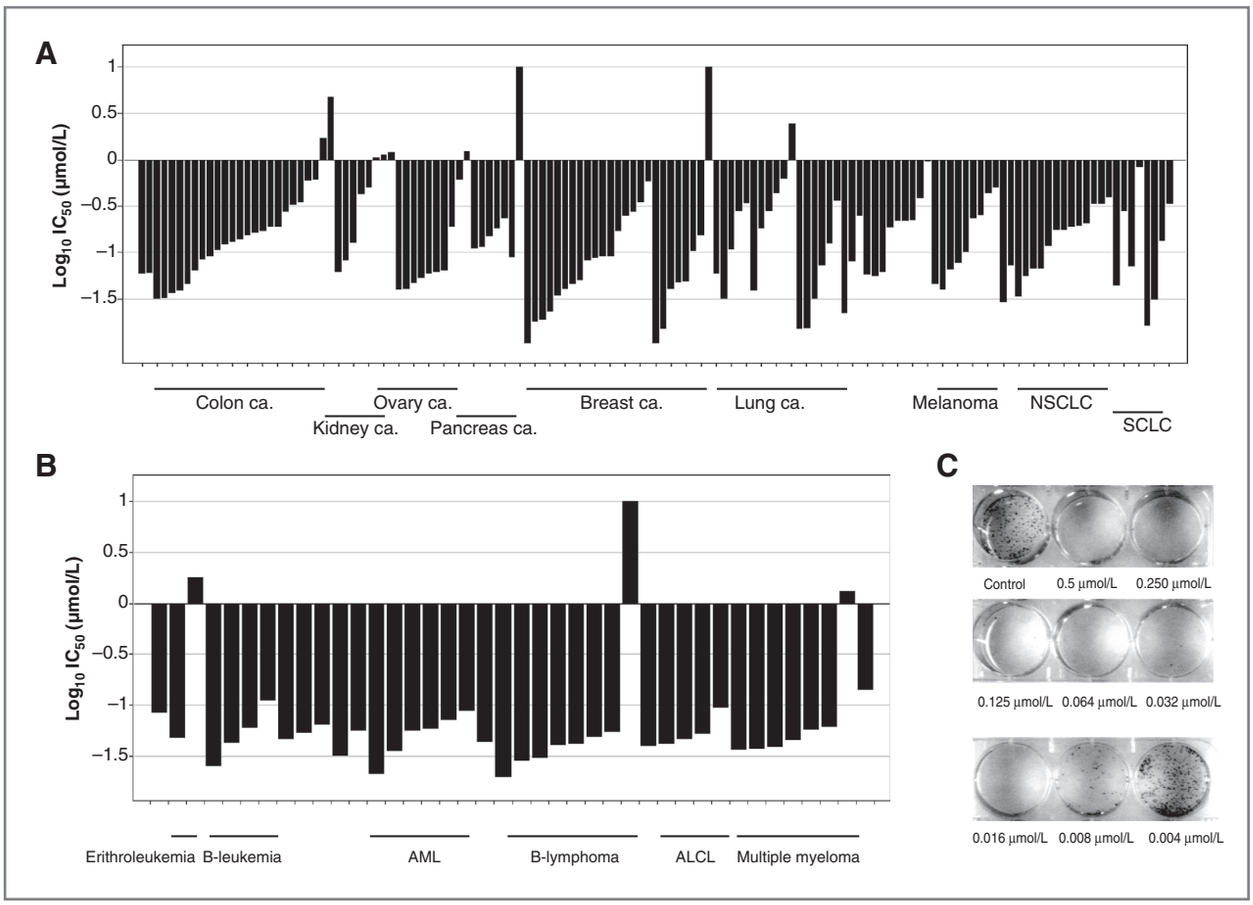

Figure 2. A, IC_{50} values for inhibition of cell proliferation after treatment with NMS-P937 in a panel of cell lines derived from solid tumors. B, IC_{50} values for inhibition of cell proliferation after treatment with NMS-P937 in a panel of cell lines derived from hematologic tumors. C, colony formation assay on HT29 colon adenocarcinoma cells treated for 72 hours with different concentrations of NMS-P937 followed by growth for 18 days in compound-free medium. ALCL, anaplastic large cell lymphoma; Ca., carcinoma.

potent on cancer cells of hematopoietic origin, where IC_{50} values more than 1 μmol/L were found only in 3 of 43 lines (Fig. 2B). Interestingly, antiproliferative activity was not affected by DNA repair deficiency status as the IC_{50} value in A2780 and A2780/cis cells, resistant to cisplatin treatment, are comparable (IC_{50} value of 0.042 and 0.048 μmol/L on A2780 and A2780/cis, respectively) and NMS-P937 is also active on cells resistant to taxol (IC_{50} value of 0.065 and 0.062 μmol/L, respectively on A2780 1A9 PTX vs. parental A2789 1A9). No correlation was observed between the antiproliferative effect and cellular doubling time or chromosomal number, which is known for the 52 cell lines belonging to the NCI 60 cell line panel.

To evaluate whether NMS-P937 was able to inhibit colony formation, HT29 cells were incubated for 72 hours in the presence of the inhibitor. The compound was then removed and cells were replated without NMS-P937 to test the ability of cells to regrow after compound removal. Concentrations down to 8 nmol/L of NMS-P937 impaired cell growth in colony-forming assays confirming the high potency of NMS-P937 (Fig. 2C).

The PLK1-associated mechanism of action of the compound was tested on several cell lines. All of them showed a homogeneous behavior in terms of cell cycle and target-related signaling modulation, in line with the expected phenotype upon inhibition of PLK1. Figure 3 shows the results obtained with A2780 cells, treated with different doses of NMS-P937 for 24 hours. Fluorescence-activated cell-sorting analysis showed a strong dose-dependent increase in cells with 4N DNA content indicative of a massive G_2–M cell-cycle block (Fig. 3A) starting from 20 nmol/L concentration of compound. To better discriminate between G_2 and M phase of the cell cycle, different cell-cycle markers were assessed by Western blotting on lysates from A2780 cells treated with different doses of NMS-P937. In late G_2 and M phases of the cell cycle, PLK1 expression usually increases, and the protein is activated by an external kinase on Thr210. Increase in phosphorylation of PLK1 on Thr210, indicative of PLK1 conversion to its active form, as well as decrease in the inhibitory phosphorylation of CDK1 on tyrosine 15 (phospho-Tyr15 CDK1) confirmed activation of both CDK1 and PLK1 and the

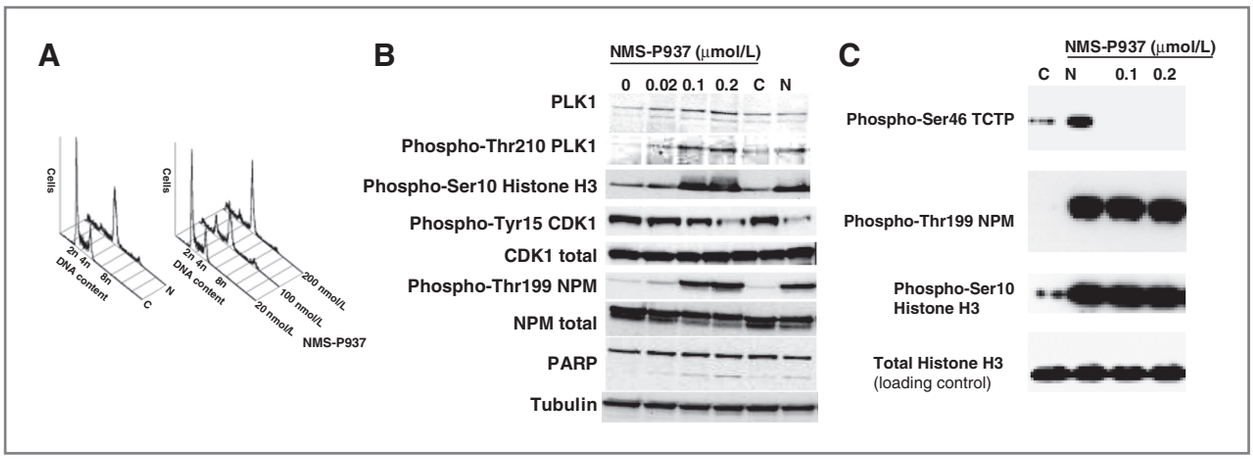

Figure 3. A, DNA content assessed by flow cytometry in A2780 cells treated with DMSO (C), nocodazole (N), or different concentrations of NMS-P937 for 24 hours. B, Western blot analysis of different cell-cycle markers of lysates from A2780 cells treated for 24 hours with different concentrations of NMS-P937 in comparison with DMSO-treated cells (C) and nocodazole-treated cells (N). Dose-dependent changes in PLK1, phospho-Thr210 PLK1, phospho-Ser10 Histone H3, phospho-Thr199 NPM, and phospho-Tyr15 Cdk1 were observed. PARP cleavage indicative of apoptosis was assessed concomitantly. Total NPM, tubulin, and total CDK1 used as loading controls. C, Western blot analysis of lysates from A2780 cells treated for 1 hour with 2 different doses of NMS-P937 in comparison with DMSO-treated cells (C) and nocodazole-treated cells (N). Phospho-Thr199 NPM and phospho-Ser10 Histone H3 as mitotic markers and phospho-Ser46 TCTP as a direct marker of PLK1 inhibition were evaluated.

initiation of mitosis. Increased phosphorylation of PLK1 on Thr210 following treatment could be consequent to attempted override of drug-induced PLK1 inhibition through a feedback mechanism of expression and phosphorylation of higher amounts of protein. Increased phosphorylation of the well-known mitotic markers Histone H3 on Ser10 and nucleophosmin on Thr199 further confirm the mitotic block obtained with the inhibitor and thus effective PLK1 inhibition (Fig. 3B). A similar pattern of marker modulation was obtained in the same cells by treatment with nocodazole, a well-known microtubule destabilizing agent able to activate mitotic spindle checkpoint and to block cells in mitosis.

Apoptosis pathway induction is instead observed as indicated by PARP cleavage at higher tested doses.

To confirm that specific inhibition of PLK1 is an early event, cells were treated for 1 hour with NMS-P937 and then the level of phosphorylation of TCTP, a direct substrate of PLK1, on Ser46 was evaluated. A clear decrease in phospho-Ser46 TCTP and an increase in phospho-Ser10 Histone H3 and phospho-Thr199 NPM were detected, confirming not only an increase in the number of mitotic cells but also a direct block of PLK1 enzymatic activity (Fig. 3C). This result is corroborated by the fact that treatment with nocodazole increased the level of phosphorylation of the 3 tested markers, indicating that TCTP is usually phosphorylated in mitosis and only direct inhibition of PLK1 activity impairs its phosphorylation.

When cellular morphology of treated cells was followed by time-lapse analysis, an increased number of rounded cells, indicative of mitotic figures, appearing few hours after the compound addition and incrementing over time was observed. At longer time points a reduced cell number and the presence of debris were indicative of cell death (Supplementary Fig. S3). To clarify whether cell death was due to apoptosis induction and occurred in mitotic cells, an ArrayScan assay was set up following phospho-Ser10 Histone H3 as a marker of mitotic cells in parallel with activated caspase-3 as apoptotic marker (Supplementary Fig. S4). After 24 hours of treatment, cells resulted positive both for phospho-Ser10 Histone H3 and caspase-3 indicating that cells enter apoptosis after a prolonged mitotic block, in agreement with what is expected from PLK1 inhibition. A quantitative ArrayScan analysis of cells positive for both phospho-Ser10 Histone H3 and caspase-3 indicated that in about 13% of cells, the 2 markers are colocalized. Induction of apoptosis from mitotic phase was also confirmed by time-lapse experiments following single-cell behavior. Single cells were followed in time after NMS-P937 treatment during the mitotic phase, and the induction of apoptotic death without restarting the cell cycle was observed. A more detailed analysis of cell morphology by confocal microscopy showed an aberrant number of spindles poles and misaligned chromosomes with caspase-3 activation in comparison with control cells (Supplementary Fig. S5). This phenotype is clearly reminiscent of that following PLK1 depletion reported in literature (17).

Comparison between normal and tumor cell lines

Because PLK1 depletion is reported to be better tolerated by normal in comparison to tumoral cells, we wanted to investigate differential potency of NMS-P937 in normal human dermal fibroblasts (NHDF) in comparison with the A2780 ovarian carcinoma cell line. Cells were treated with different concentrations of NMS-P937 and the compound was then removed after different incubation times, ranging from 1 to 72 hours. Cells were then left to grow in the absence of NMS-P937. At least 10-fold difference in IC_{50} values was observed at all tested time points, with

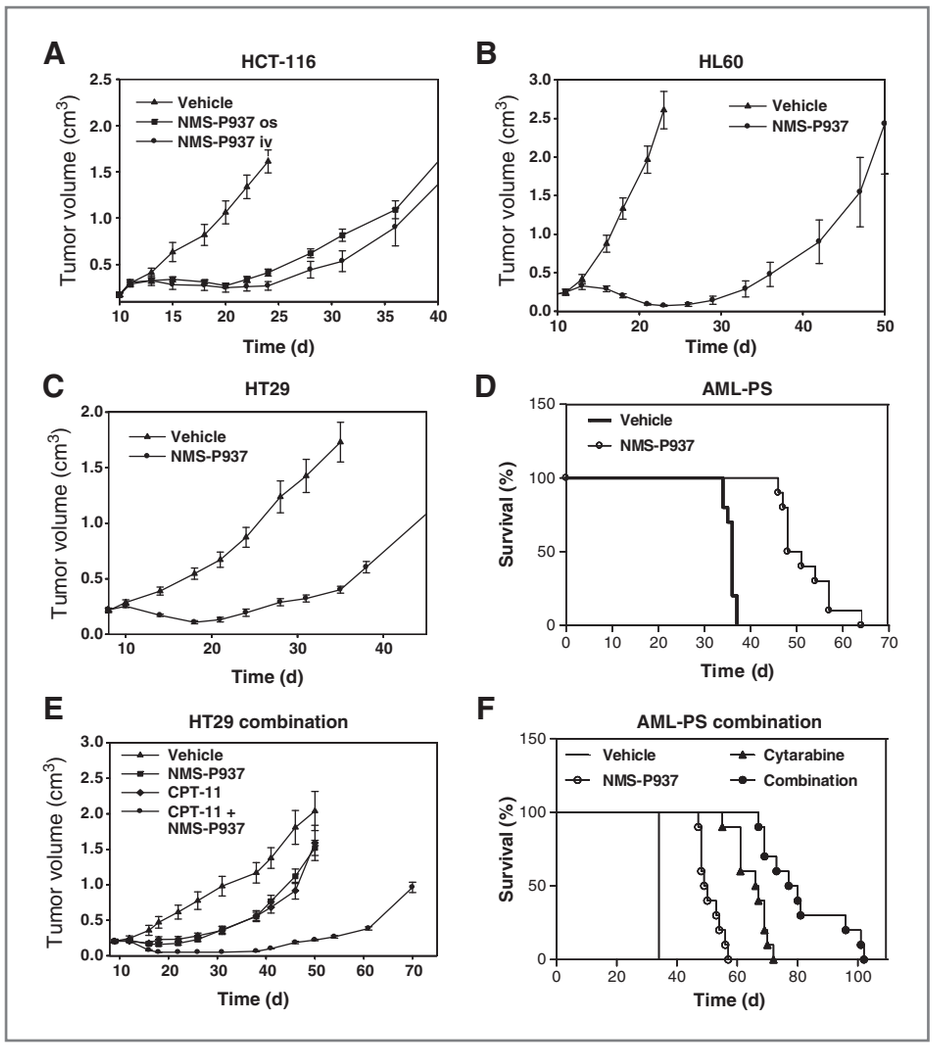

Figure 4. *In vivo* efficacy of NMS-P937 in subcutaneous xenograft models. A, HCT116 human colon adenocarcinoma–bearing mice treated with NMS-P937 either i.v. with 2 cycles of 3 consecutive days at 45 mg/kg twice a day or orally (os) for 8 consecutive days at 60 mg/kg. HL60 human promyelocytic leukemia (B) and HT29 human colon adenocarcinoma–bearing (C) mice treated orally with 60 mg/kg NMS-P937 for 10 consecutive days. D, disseminated AML-bearing mice treated orally with 120 mg/kg NMS-P937 for 2 days repeated for 5 cycles with a 5-day rest. E, HT29-bearing mice treated with the combination of NMS-P937 and CPT11. NMS-P937 was given orally at 45 mg/kg for 2 cycles of 3 consecutive days with 1-day rest. CPT11 was administered i.v. at 45 mg/kg every 4 days for 3 times. The combination was given at the same schedule, doses, and routes of the single agents. F, disseminated AML-bearing mice treated with the combination of NMS-P937 and cytarabine. NMS-P937 was given orally at 120 mg/kg for 2 days repeated for 4 cycles with a 10-day rest. Cytarabine was administered intraperitoneally at 75 mg/kg for 5 cycles of 5 consecutive days with 7-day rest. The combination was given at the same schedule, doses, and routes of the single agents.

fibroblasts being the least sensitive. At early time points, the compound resulted to be poorly active even in A2780, whereas increasing treatment time up to 24 hours, and thus allowing more cells to enter mitosis, resulted in potency of NMS-P937 in this cell line comparable with that measured at 72 hours treatment. In NHDF, the compound was found to be very poorly active at 24 hours exposure, and only upon further increased treatment times could an IC_{50} value in the high nanomolar range be observed. (Supplementary Fig. S7A). To better understand whether the different sensitivities of A2780 and NHDF is linked to a different MoA of NMS-P937, the cell lines were treated with NMS-P937 at 2 different doses (0.5 and 1 μmol/L) for 8 hours, then the compound was withdrawn, and cells were replated and allowed to grow for 24 and 48 hours in absence of drug. A clear difference following NMS-P937 treatment was again observed between A2780 and NHDF, with a slight reduction in cell number for NHDF, compared with a strong reduction for A2780 (Supplementary Fig. S7B). In both cell lines, mitotic block and positivity for pH2AX, indicative of DNA damage, was observed after 8 hours treatment with the compound. However, following washout, NHDF recovered completely, whereas A2780 continue to be positive for mitotic markers and for pH2AX, indicating that after initial injury induced by NMS-P937, normal cells are able to repair the damage and restart a normal cell cycle, whereas tumoral cells are committed to death, remaining blocked for a prolonged period in mitosis, with an activated DNA damage signal (Supplementary Fig. S7C). These data, while limited to 2 cell lines, are fully consistent with previous reports, and are indicative of potential selectivity of PLK1 inhibitors for proliferating tumoral cells in comparison with normal cells.

Antitumor activity *in vivo*

On the basis of *in vitro* activity, the compound was tested in different human xenograft tumors implanted in immunodeficient mice. Because of its pharmacokinetic properties (Supplementary Table S4), NMS-P937 is

suitable for intravenous or oral administration. In initial studies, HCT116 (human colon adenocarcinoma)-bearing mice were treated either intravenously, with a schedule of 2 cycles of 3 consecutive days at 45 mg/kg twice a day, or orally for 8 consecutive days at 60 mg/kg. With both schedules, a good antitumor activity (TGI, 83% and 79% intravenously and orally, respectively) was obtained with a minimal body weight loss (Fig. 4A). Because both administration routes inhibited tumor growth to a comparable degree, further *in vivo* studies were conducted by oral treatment using different xenograft models and refining the schedule. An increase of TGI up to 89% was obtained in the HCT116 xenograft model prolonging the treatment at 60 mg/kg for 10 days (data not shown). Similar results were obtained also in 2 other colon carcinomas, HT29 (Fig. 4C) and Colo205, and in an ovarian cancer A2780 (data not shown). The same schedule applied to the subcutaneously implanted HL60 human acute leukemia model–induced tumor regression in all treated animals, which was maintained for about 10 days after drug suspension (Fig. 4B). On the basis of the significant TGI (98%) obtained in the subcutaneously implanted HL60 model, NMS-P937 efficacy was also explored in a disseminated model of a human primary leukemia, which might more closely resemble the pathogenesis of the disease in man. For this purpose, AML cells (AML-PS) with a normal karyotype derived from a patient were used. A different schedule of administration for NMS-P937 was evaluated and a 2-day treatment at the higher dose of 120 mg/kg, simulating an induction dose such as is clinically used for hematologic malignancies, was tested. As shown in Fig. 4D, NMS-P937 administered at 120 mg/kg orally for 2 days repeated for 5 cycles with a 5-day rest, showed a significant increase ($P < 0.0001$) in median survival time (50 days) compared with the vehicle (36 days).

Recently a role for PLK1 in DNA damage adaptation and cell-cycle restart has been reported (25). To evaluate whether NMS-P937 is able to synergize with DNA-damaging agents, the compound was tested in 2 different xenograft models in combination with cytarabine or irinotecan (CPT11). The combination of NMS-P937 (120 mg/kg given for 4 cycles of 2 consecutive days with 10-day rest) and cytarabine (75 mg/kg for 4 cycles of 5 consecutive days with 7-day rest) in the disseminated leukemia model AML-PS was well tolerated and clearly showed increased mice survival. In fact, a median survival time of 79 days for animals treated with the combination was obtained in comparison with 34 days for vehicle or 50 and 67 days for NMS-P937 and cytarabine, respectively, as single agents. Of note, with the combination 3 of 10 animals survived more than 90 days (Fig. 4F). The combination of NMS-P937 and CPT11 was tested on HT29 human colon adenocarcinoma–bearing mice. The animals were treated with NMS-P937 orally at 45 mg/kg for 2 cycles of 3 consecutive days with 1-day rest or with CPT11 at 45 mg/kg intraperitoneally every 4 days for 3 times (day 1, 5, and 9) and with the combination of the 2 agents. NMS-P937 and CPT11 alone inhibited tumor growth of 72% and 64%, respectively. The combination of the 2 agents resulted in a strikingly synergistic effect with regression of all tumors, that lasted for 20 days after drug suspension (Fig. 4E). Also in this model, the combination was well tolerated.

In vivo mechanism of action

To show that NMS-P937 inhibits PLK1 activity *in vivo* and that its mechanism of action correlates with suppression of tumor growth, A2780 xenograft tumors were collected at different time points (2, 6, 12, and 24 hours) after a single oral treatment with 3 doses of the compound (60, 90, and 120 mg/kg). Tumors were analyzed by

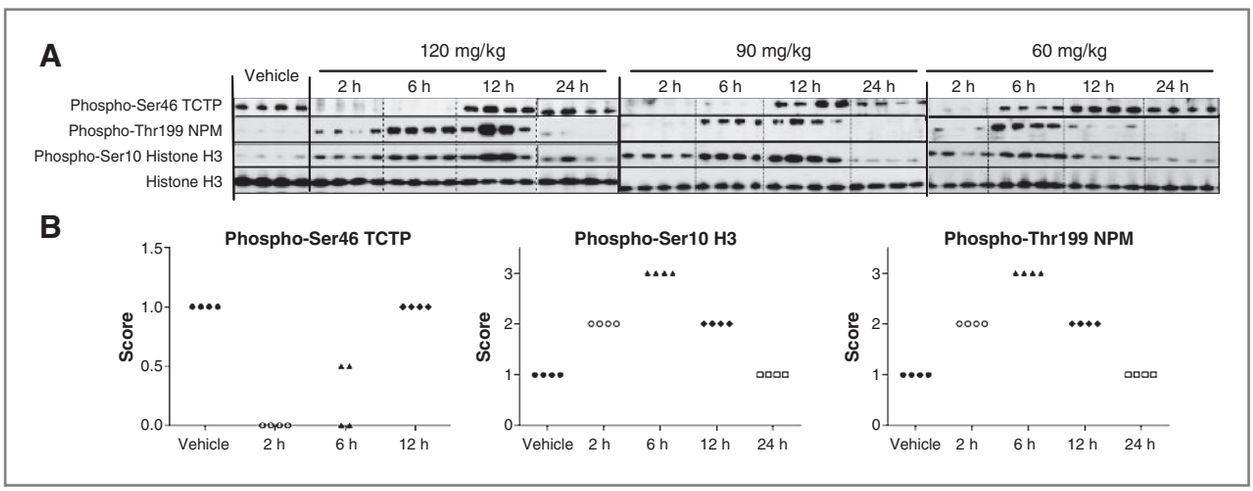

Figure 5. *In vivo* mechanism of action of NMS-P93. A2780 tumor–bearing mice were treated with single oral doses of NMS-P937 and sacrificed at the indicated time points after administration. A, modulation of phospho-Ser46 TCTP, phospho-Ser10 Histone H3, and phospho-Thr199 NPM induced by single administration of different doses of NMS-P937 (60, 90, or 120 mg/kg) was evaluated in tumors by Western blotting at different time points. B, modulation of the same biomarkers after treatment with NMS-P937 at 60 mg/kg was evaluated in tumors by immunohistochemistry.

Western blot analysis evaluating levels of phospho-Ser46 TCTP, as the PLK1 direct substrate, phospho-Ser10 Histone H3 and phospho-Thr199 NPM as mitosis markers. At 60 mg/kg, phospho-Ser46 TCTP levels decreased within 2 hours after treatment, whereas recovery started at 6 hours and was complete at 12 hours. At higher doses, phospho-TCTP downregulation was maintained for up to 6 hours, with recovery at 12 hours (Fig. 5A). Upregulation of mitotic markers instead lasted for 6 to 12 hours indicating that, after a reversible PLK1 inhibition, tumors remain blocked in mitosis for a prolonged period.

In the same experiment tumor samples from mice treated with the dose of 60 mg/kg were collected 2, 6, 12, and 24 hours after treatment and analyzed also by immunohistochemistry.

Tumors treated with NMS-P937 showed a decrease of cells positive for phospho-Ser46 TCTP as assessed by immunohistochemistry. No positive cells were observed at 2 hours after treatment, whereas after 6 hours a few positive cells were present and by 12 hours after treatment the level of phospho-Ser46 TCTP was comparable with the tumors from vehicle-treated animals (Fig. 5B).

On the contrary, phospho-Ser10 Histone H3 and phospho-Thr199 NPM–positive cells were already increased by 2 hours, and further increased at 6 hours (Fig. 5B), but had started declining by 12 hours after the treatment and returned to vehicle-treated levels at 24 hours, confirming the results obtained by Western blot and that show mitotic arrest in treated tumor tissues. Representative images of PLK1 biomarker expression are reported in Supplementary Fig. S8.

Pharmacokinetics and pharmacodynamics

Pharmacokinetic parameters were measured in mouse, rat, dog, and monkeys. After intravenous administration, the compound showed moderate plasma clearance, with a high volume of distribution in all species, suggesting extensive tissue distribution and good oral bioavailability, with $F = 25\%, 100\%, 63\%$, and 35% in mouse, rat, dog, and monkey, respectively (Supplementary Table S4).

A pharmacokinetic and pharmacodynamic approach, based on a previously described model (26), was applied to the efficacy data obtained in HL60 tumor–bearing mice. This method, which links plasma concentrations of the anticancer compound to effects on tumor growth, provides quantitative estimates of *in vivo* potency through the determination of 2 specific parameters: K_2 and C_t. K_2 can be regarded as a drug-specific measurement of potency of the compound. The C_t value provides an estimate of the steady state drug concentration in plasma required for tumor regression and eventually tumor eradication. The estimated C_t value for NMS-P937 in the HL-60 model was 0.43 μmol/L indicative of a highly potent compound (Fig. 6, Table 2).

Discussion

Drugs interfering with the normal progression of mitosis such as the taxanes and vinca alkaloids are amongst the most successful chemotherapeutic compounds currently used for anticancer treatment. These drugs are microtubule-binding compounds that inhibit the function of the mitotic spindle to halt the cell cycle in mitosis and to induce apoptosis in tumor cells. However, these agents act not only on proliferating tumor cells, but exhibit significant side effects on nonproliferating cells including neurons, which are highly dependent on intracellular transport processes mediated by microtubules (27).

In fact peripheral neuropathy is reported as a dose-limiting toxicity with different microtubule-binding agents and grade more than 2 neuropathy is noted in up to 30% of patients receiving paclitaxel (28). Therefore, there is a particular interest in developing novel antimitotic drugs that target nonmicrotubule structures (29).

PLK1 is a master regulator of mitosis that is expressed in all proliferating cells and overexpressed in a number of malignant tumors. PLK1 inhibition is considered a promising new approach for targeting mitosis (30) and the first inhibitors targeting this kinase have reached clinical trials. Among these, BI-2536 (31) and BI-6727 (32) completed phase I studies showing acceptable safety margins and

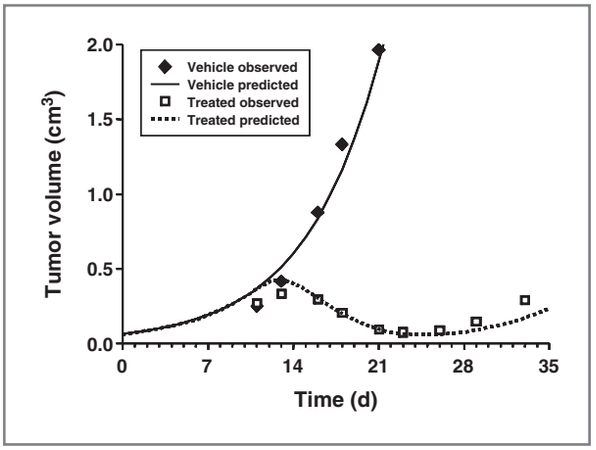

Figure 6. Pharmacokinetic/pharmacodynamic model of HL60 xenografts. Observed and predicted tumor volume was fitted with tumor growth curves obtained in nude mice–bearing HL60 xenograft tumors treated orally with NMS-P937 or vehicle at 60 mg/kg for 10 days.

Table 2. Drug-specific parameters of the pharmacokinetic- and pharmacodynamic-applied models are reported

Parameter	Value	Coefficient of variance (%)
K_1, L/h	0.035	25.4
K_2, L/μmol/L/h	0.016	9.14
λ_0, L/h	0.007	8.59
λ_1, g/h	0.012	15.0
L_0, G	0.060	24.1
C_t, μmol/L	0.433	

with preliminary evidence of antitumor activity, justifying further development in phase II studies.

In this study, we have described the activity of NMS-P937 a new, highly potent, orally available small-molecule PLK1 inhibitor.

Main features differentiating NMS-937 from compounds undertaking phase II clinical trials consist in PLK1 selectivity and oral bioavailability.

BI-2536 and BI-6727 are in fact highly potent not only on PLK1 (IC_{50} value 0.83 and 0.87 nmol/L, respectively) but also on PLK2 (IC_{50} value 3.5 and 5 nmol/L, respectively) and PLK3 (IC_{50} value 9 and 56 nmol/L, respectively). The functional role of these 2 additional PLK family members is still elusive, however, PLK2 and PLK3 emerge as important mediators of stress phenotype or oxidative damage and their expression in detected in the central nervous system (33).

PLK2 has been suggested to be a tumor suppressor gene *in vivo*, due to the fact that deletion of the long arm of chromosome 5, where the PLK2 gene is located, is frequent in AML and myelodysplastic syndrome (34). Large scale miRNA studies in AML further corroborated a tumor suppressor role for PLK2 (35). Evidence of a tumor suppressor function of PLK2 in hematologic diseases is also reported for B-cell malignancies (36).

A central nervous system localization and a tumor suppressor role are reported also for PLK3. Nevertheless PLK3 seems to be differentially regulated compared with PLK1. In particular it is downregulated in tumor tissues and it is upregulated after DNA damage or different type of cellular stress. Mice deficient for PLK3 are viable but develop tumors (37).

In light of all these considerations a PLK1-specific inhibitor such as NMS-P937 might show a better long-term safety profile in terms of effects on nonproliferating tissues due to off-targets effects on additional members of the polo kinase family.

A second differentiating feature of NMS-P937 is oral administration. Indeed, both BI-2536 and BI-6727 are administered intravenously with intermittent scheduling in the clinic, and a number of clinical trials have been undertaken with the aim of reaching an optimal therapeutic index. As expected, dose-limiting toxicities are seen on proliferating normal cells, with neutropenia being the most pronounced.

Despite proven activity in both *in vitro* and *in vivo* preclinical models, partial responses with advanced PLK inhibitors in clinical trials are very limited, possibly due to a narrow therapeutic window and lack of dosing flexibility for these compounds. No pharmacodynamic biomarkers have been evaluated in the clinic up to now, limiting the possibility to have a clear pharmacodynamic model (38). The only model reported to date for supporting schedule optimization is based retrospectively on neutropenic effects induced by BI-2536 in phase I patients (39).

The availability of a clear direct marker of PLK1 activity such as phospho-Ser46 TCTP that will be followed in the ongoing clinical trial for NMS-P937 could pave the way for better toxicokinetic and pharmacokinetic modeling aimed at identifying the most promising schedules of administration. In addition, oral bioavailability is a factor that might permit higher schedule flexibility.

This approach might allow exposure to the drug to be modulated on a personalized basis, which ideally would result in a sufficient target inhibition to drive tumor cells to apoptosis while minimizing effects on normal tissues.

In addition, the identification of tumor types peculiarly sensitive to PLK1 inhibition as well as the identification of combination with agent with different spectrum of toxicities will help in increasing the therapeutic window for these new targeted agents.

The possibility to use PLK1 inhibitors in a KRAS-mutated setting could be considered on the basis of synthetic lethality between PLK1 depletion and KRAS mutation.

Genome-wide RNA interference screen in an isogenic pair of DLD-1 colorectal cancer cell lines showed selective growth impairment of KRAS-mutated cells upon knockdown of PLK1 (40). Higher sensitivity is possibly due to a mitotic stress caused by KRAS mutation delaying mitotic progression and rendering cells more dependent on key mitotic proteins and as consequence to drugs interfering with mitotic progression. This finding might represent a basis for defining a specific patient population in colon cancer that can benefit from therapy with PLK1 inhibitors.

In addition, the reported role for PLK1 in cell-cycle progression recovery after DNA damage and literature data indicating higher sensitivity of TP53-negative cell lines to PLK1 inhibition (41) would support the rationale for testing a combination of radiotherapy or DNA-damaging agents and PLK1 inhibitors, particularly in a patient population with deficient TP53 function. This hypothesis is supported by our preclinical experiments where the combination of NMS-P937 with DNA-damaging agents such as irinotecan (CPT11) and cytarabine resulted in a clear synergistic effect.

The availability of an oral drug suitable to be used for prolonged treatment periods, once safety profile will be clearly defined in phase I studies, will also open up the possibility of use PLK1 inhibitors for maintenance therapy (42).

The high flexibility of agents such as NMS-P937, that show *in vivo* activity when administered orally on a range of schedules from twice weekly to prolonged once daily should facilitate the identification of optimal combination dosing schedules, the management of overlapping toxicities, and the exploration of maintenance therapy. For these reasons, NMS-P937 with its unique PLK1 selectivity profile coupled with oral bioavailability warrants systematic clinical evaluation.

Disclosure of Potential Conflicts of Interest

All authors are employees of Nerviano Medical Sciences s.r.l. and Accelera s.r.l.

In Memoriam

The authors dedicate the manuscript to the memory of Valter Croci, friend and colleague who greatly contributed to the development of the product.

Authors' Contributions

Conception and design: B. Valsasina, I. Beria, E. Felder, A. Galvani, A. Isacchi

Development of methodology: C. Alli, D. Ballinari, A. Ciavolella, U. Cucchi, E. Felder, A. Galvani, M.L. Giorgini, F. Sola

Acquisition of data (provided animals, acquired and managed patients, provided facilities, etc.): C. Alli, R. Alzani, D. Ballinari, A. Casolaro, A. Ciavolella, A. Isacchi, E. Pesenti

Analysis and interpretation of data (e.g., statistical analysis, biostatistics, computational analysis): I. Beria, C. Alli, R. Alzani, A. Isacchi

Writing, review, and/or revision of the manuscript: B. Valsasina, I. Beria, C. Alli, E. Felder, A. Galvani, A. Isacchi, J. Moll

Study supervision: B. Valsasina, E. Felder, E. Pesenti

Acknowledgments

The authors thank all their colleagues in the Cell Biology, Biotechnology, Chemistry, Pharmacology, and Toxicology Departments for their contributions and Daniele Donati for the critical review of the manuscript.

The costs of publication of this article were defrayed in part by the payment of page charges. This article must therefore be hereby marked *advertisement* in accordance with 18 U.S.C. Section 1734 solely to indicate this fact.

Received September 28, 2011; revised January 9, 2012; accepted January 27, 2012; published OnlineFirst February 7, 2012.

References

1. Strebhardt K. Multifaceted polo-like kinases: drug targets and anti-targets for cancer therapy. Nat Rev Drug Discov 2010;9:643–60.
2. Barr FA, Sillje HH, Nigg EA. Polo-like kinases and the orchestration of cell division. Nat Rev Mol Cell Biol 2004;5:429–40.
3. Gray PJ Jr, Bearss DJ, Han H, Nagle R, Tsao MS, Dean N, et al. Identification of human polo-like kinase 1 as a potential therapeutic target in pancreatic cancer. Mol Cancer Ther 2004;3:641–6.
4. Takahashi T, Sano B, Nagata T, Kato H, Sugiyama Y, Kunieda K, et al. Polo-like kinase 1 (PLK1) is overexpressed in primary colorectal cancers. Cancer Sci 2003;94:148–52.
5. Weichert W, Schmidt M, Gekeler V, Denkert C, Stephan C, Jung K, et al. Polo-like kinase 1 is overexpressed in prostate cancer and linked to higher tumor grades. Prostate 2004;60:240–5.
6. Weichert W, Denkert C, Schmidt M, Gekeler V, Wolf G, Kobel M, et al. Polo-like kinase isoform expression is a prognostic factor in ovarian carcinoma. Br J Cancer 2004;90:815–21.
7. Weichert W, Kristiansen G, Winzer KJ, Schmidt M, Gekeler V, Noske A, et al. Polo-like kinase isoforms in breast cancer: expression patterns and prognostic implications. Virchows Arch 2005;446: 442–50.
8. Knecht R, Elez R, Oechler M, Solbach C, von Ilberg C, Strebhardt K. Prognostic significance of polo-like kinase (PLK) expression in squamous cell carcinomas of the head and neck. Cancer Res 1999;59:]2794–7.
9. Salvatore G, Nappi TC, Salerno P, Jiang Y, Garbi C, Ugolini C, et al. A cell proliferation and chromosomal instability signature in anaplastic thyroid carcinoma. Cancer Res 2007;67:10148–58.
10. Schmit TL, Zhong W, Setaluri V, Spiegelman VS, Ahmad N. Targeted depletion of Polo-like kinase (Plk) 1 through lentiviral shRNA or a small-molecule inhibitor causes mitotic catastrophe and induction of apoptosis in human melanoma cells. J Invest Dermatol 2009;129:2843–53.
11. Ikezoe T, Yang J, Nishioka C, Takezaki Y, Tasaka T, Togitani K, et al. A novel treatment strategy targeting polo-like kinase 1 in hematological malignancies. Leukemia 2009;23:1564–76.
12. Renner AG, Dos Santos C, Recher C, Bailly C, Creancier L, Kruczynski, et al. Polo-like kinase 1 is overexpressed in acute myeloid leukemia and its inhibition preferentially targets the proliferation of leukemic cells. Blood 2009;114:659–62.
13. Mito K, Kashima K, Kikuchi H, Daa T, Nakayama I, Yokoyama S. Expression of Polo-Like Kinase (PLK1) in non-Hodgkin's lymphomas. Leuk Lymphoma 2005;46:225–31.
14. Elez R, Piiper A, Kronenberger B, Kock M, Brendel M, Hermann E, et al. Tumor regression by combination antisense therapy against Plk1 and Bcl-2. Oncogene 2003;22:69–80.
15. Matthess Y, Kappel S, Spankuch B, Zimmer B, Kaufmann M, Strebhardt K. Conditional inhibition of cancer cell proliferation by tetracycline-responsive, H1 promoter-driven silencing of PLK1. Oncogene 2005;24:2973–80.
16. Seong YS, Kamijo K, Lee JS, Fernandez E, Kuriyama R, Miki T, et al. A spindle checkpoint arrest and a cytokinesis failure by the dominant-negative polo-box domain of Plk1 in U-2 OS cells. J Biol Chem 2002;277:32282–93.
17. Liu X, Lei M, Erikson RL. Normal cells, but not cancer cells, survive severe Plk1 depletion. Mol Cell Biol 2006;26:2093–108.
18. Seeburg DP, Pak D, Sheng M. Polo-like kinases in the nervous system. Oncogene 2005;24:292–8.
19. Lens SM, Voest EE, Medema RH. Shared and separate functions of polo-like kinases and aurora kinases in cancer. Nat Rev Cancer 2010;10:825–41.
20. Beria I, Valsasina B, Brasca MG, Ceccarelli W, Colombo M, Cribioli, et al. 4,5-Dihydro-1*H*-pyrazolo[4,3-*h*]quinazolines as potent and selective Polo-like kinase 1 (PLK1) inhibitors. Bioorg Med Chem Lett 2010;20:6489–94.
21. Beria I, Ballinari D, Bertrand JA, Borghi D, Bossi RT, Brasca MG, et al. Identification of 4,5-dihydro-1*H*-pyrazolo[4,3-*h*]quinazoline derivatives as a new class of orally and selective Polo-like kinase 1 inhibitors. J Med Chem 2010;53:3532–51.
22. Cucchi U, Gianellini LM, De Ponti A, Sola F, Alzani R, Patton V, et al. Phosphorylation of TCTP as a marker for polo-like kinase-1 activity *in vivo*. Anticancer Res 2010;30:4973–85.
23. Radaelli E, Ceruti R, Patton V, Russo M, Degrassi A, Croci V, et al. Immunohistopathological and neuroimaging characterization of murine orthotopic xenograft models of glioblastoma multiforme recapitulating the most salient features of human disease. Histol Histopathol 2009;24:879–91.
24. Beria I, Brasca MG, Caruso M, Ceccarelli W, Fachin G, Fasolini M, et al. NMS-P937, a 4,5-dihydro-1*H*-pyrazolo[4,3-*h*]quinazoline derivative as potent and selective Polo-like kinase 1 inhibitor. Bioorg Med Chem Lett 2011;21:2969–74.
25. Van Vugt MA, Medema RH. Checkpoint adaptation and recovery: back with Polo after the break. Cell Cycle 2004;3:1383–6.
26. Rocchetti M, Simeoni M, Pesenti E, De Nicolao G, Poggesi I. Predicting the active doses in humans from animal studies: a novel approach in oncology. Eur J Cancer 2007;43:1862–8.
27. Dumontet C, Jordan MA. Microtubule-binding agents: a dynamic field of cancer therapeutics. Nat Rev Drug Discov 2010;9:790–803.
28. Lee JJ, Swain SM. Peripheral neuropathy induced by microtubule-stabilizing agents. J Clin Oncol 2006;24:1633–42.
29. Jackson JR, Patrick DR, Dar MM, Huang PS. Targeted anti-mitotic therapies: can we improve on tubulin agents? Nat Rev Cancer 2007;7:107–17.
30. Schoffski P. Polo-like kinase (PLK) inhibitors in preclinical and early clinical development in oncology. Oncologist 2009;14:559–70.
31. Hofheinz RD, Al-Batran SE, Hochhaus A, Jager E, Reichardt VL, Fritsch H, et al. An open-label, phase I study of the polo-like kinase-1 inhibitor, BI 2536, in patients with advanced solid tumors. Clin Cancer Res 2010;16:4666–74.
32. Rudolph D, Steegmaier M, Hoffmann M, Grauert M, Baum A, Quant J, et al. BI 6727, a Polo-like kinase inhibitor with improved pharmacokinetic profile and broad antitumor activity. Clin Cancer Res 2009;15:3094–102.

33. Winkles JA, Alberts GF. Differential regulation of polo-like kinase 1, 2, 3, and 4 gene expression in mammalian cells and tissues. Oncogene 2005;24:260–6.
34. Benetatos L, Dasoula A, Hatzimichael E, Syed N, Voukelatou M, Dranitsaris G, et al. Polo-like kinase 2 (SNK/PLK2) is a novel epigenetically regulated gene in acute myeloid leukemia and myelodysplastic syndromes: genetic and epigenetic interactions. Ann Hematol 2011;9:1037–45.
35. Li Z, Lu J, Sun M, Mi S, Zhang H, Luo RT, et al. Distinct microRNA expression profiles in acute myeloid leukemia with common translocations. Proc Natl Acad Sci U S A 2008;105:15535–40.
36. Syed N, Smith P, Sullivan A, Spender LC, Dyer M, Karran L, et al. Transcriptional silencing of Polo-like kinase 2 (SNK/PLK2) is a frequent event in B-cell malignancies. Blood 2006;107:250–6.
37. Yang Y, Bai J, Shen R, Brown SA, Komissarova E, Huang, et al. Polo-like kinase 3 functions as a tumor suppressor and is a negative regulator of hypoxia-inducible factor-1 alpha under hypoxic conditions. Cancer Res 2008;68:4077–85.
38. Olmos D, Swanton C, de Bono J. Targeting polo-like kinase: learning too little too late? J Clin Oncol 2008;26:5497–9.
39. Soto E, Staab A, Freiwald M, Munzert G, Fritsch H, Doge C, et al. Prediction of neutropenia-related effects of a new combination therapy with the anticancer drugs BI 2536 (a Plk1 inhibitor) and pemetrexed. Clin Pharmacol Ther 2010;88:660–7.
40. Luo J, Emanuele MJ, Li D, Creighton CJ, Schlabach MR, Westbrook TF, et al. A genome-wide RNAi screen identifies multiple synthetic lethal interactions with the Ras oncogene. Cell 2009;137:835–48.
41. Sur S, Pagliarini R, Bunz F, Rago C, Diaz LA Jr, et al. A panel of isogenic human cancer cells suggests a therapeutic approach for cancers with inactivated p53. Proc Natl Acad Sci U S A 2009;106:3964–9.
42. Christoph DC, Schuler M. Polo-like kinase 1 inhibitors in mono- and combination therapies: a new strategy for treating malignancies. Expert Rev Anticancer Ther 2011;11:1115–30.